Super-resolution imaging reveals dynamic skeletal cytoophidia

Yifan Fang[1], Yi-Lan Li[1], Xiao-Ming Li[1] and Ji-Long Liu[1,2,*]

[1]School of Life Science and Technology, ShanghaiTech University, Shanghai, China

[2]Department of Physiology, Anatomy and Genetics, University of Oxford, Oxford, OX1 3PT, United Kingdom

*Correspondence: liujl3@shanghaitech.edu.cn; jilong.liu@dpag.ox.ac.uk

ABSTRACT

CTP synthase (CTPS) can form filamentous structures termed cytoophidia in cells from all three domains of life. In order to study the mesoscale structure of cytoophidia, we perform fluorescence recovery after photobleaching (FRAP) and stimulated emission depletion (STED) microscopy in human cells. By using EGFP dimeric tag, as a tool to explore the physical properties of cytoophidia, we find that cytoophidia are dynamic and skeletal. The skeletal structure of CTPS cytoophidia may provide space for other components such as IMPDH. In addition, we observe CTPS granules with tentacles.

Keywords: CTP synthase; cytoophidium; fluorescence recovery after photobleaching (FRAP); Stimulated emission depletion (STED)

INTRODUCTION

In addition to organelles with membrane, proteins with important functions in the cell can also be compartmentalized into membraneless organelles. Protein compartmentalization, like droplets, can be assembled driven by physical forces in cells (Brangwynne et al., 2009). CTP synthase (CTPS), a metabolic enzyme for *de novo* synthesis of CTP, was found to form filament-like compartmentalization in cells called cytoophidia (Ingerson-Mahar et al., 2010; Liu, 2010; Noree et al., 2010). Cytoophidia are conserved in evolution (Liu, 2016). A glutamine analog, 6-diazo-5-oxo-L-norleucine (DON), promotes cytoophidia formation in *Drosophila* and human cells (Chen et al., 2011). DON binds CTPS with covalent bonds (Zhou et al., 2021). Many metabolic enzymes that can form cytoophidia are related to glutamine and NH_3 metabolism, including CTPS, IMPDH (Ji et al., 2006). It was reported that there is an interaction between CTPS and IMPDH (Chang et al., 2018). The function of cytoophidia may be closely related to glutamine and NH_3 metabolism.

CTPS can be assemble into thin filaments in vitro, and the structures of CTPS filaments at near-atomic resolution have been solved by cryo-EM (Lynch et al., 2017; Zhou et al., 2019). However, nanometer scale CTPS filaments are different from micron scale cytoophidia observed under confocal microscopy. How cytoophidium filaments assembles intobig micron scale cytoophidia is still

unclear. That is to say, the physical properties of cytoophidia remain to be explored and the mesoscale insights must be gained

To study cytoophidium properties in human cell lines, we carried out fluorescence recovery after photobleaching (FRAP) microscopy to study the dynamic characteristics and stimulated emission depletion (STED) microscopy to study the super-resolution structure. By measuring the intensity and recovery speed of bleaching ROI, we can quantify the relative dynamic characteristics of cytoophidia with different treatments. STED allows fluorescence imaging to achieve a resolution of 50 to 70 nm. EGFP tag is dimeric (Shaner et al., 2005), which can provide a simple force for tagged hCTPS1 to form a cytoophidium-like condensate (Chang et al., 2018). We used the EGFP tag as an excellent tool to study the dynamic characteristics and structures of cytoophidia. The mutation H355A in CTPS was found to disassemble CTPS filaments (Zhou et al., 2019). CTPS^{H355A} and EGFP tag enable us to study the mechanism of CTPS assembly into filaments rather than granules.

We find that the H355 site of CTPS is an important connecting point for filament formation, rather than just providing forces only. We also find that cytoophidia are highly dynamic and structured like a skeleton. In terms of dynamic characteristics and super-resolution structures, typical cytoophidia and hCTPS1-EGFP cytoophidium-like condensates are different. In addition, we

also capture another type of CTPS structure, that is, the CTPS granule with tentacles.

RESULTS

Assembly of CTPS filaments into cytoophidia

The cytoophidium is a compartment of metabolic enzymes, such as filamentous CTPS, which can be observed under confocal microscopy (Ingerson-Mahar et al., 2010; Liu, 2010; Noree et al., 2010). In vitro experiments showed that CTPS can also form filaments building from tetramer units (Lynch et al., 2017; Zhou et al., 2019). In human cells, CTPS can be assembled into cytoophidia under DON treatment or glutamine deprivation. In this study, we did not distinguish hCTPS1 and hCTPS2. We found that after DON treatment, hCTPS1 can form granules in 293T cells with hCTPS1 over-expression (Figure 1A and B). When we observed living cells, CTPS granules existed in a small population of cells. CTPS granules can exist in the same cell with cytoophidia (Figure 1A-C).

How CTPS filaments are arranged in cytoophidia remains unclear. To conceive the arrangement model from CTPS filaments to cytoophidia, we constructed hCTPS1 overexpression vectors with different fluorescence proteins and different mutations (Supplemental Table S1). In order to show and evaluate the effect of exogenous overexpression protein on the experiment, we compared the protein levels of overexpressed hCTPS1 and endogenous hCTPS1/2 (Figure 1D), and tested the transfection efficiencies (Figure 1E and F). In transfection positive cells, exogenous hCTPS1 was approximately twice as

much as endogenous hCTPS1/2 (Figure 1G).

EGFP is a weak dimer (Shaner et al., 2005). Overexpression of hCTPS1-EGFP forms cytoophidium-like condensates in 293T cells (Figure 1H). The force of forming dimer between EGFP pulls hCTPS1 together, and hCTPS is assembled into filaments. The hCTPS filaments may be compressed together by a simple force between EGFP(Figure 1C). The hCTPS1-EGFP group was a control for cytoophidium induction. CTPS1 with H355A mutation disassembles cytoophidia. We found that overexpressed hCTPS1^{H355A}-EGFP could not form cytoophidia in 293T cells (Figure 1H).

Dynamic equilibrium of cytoophidia

To test the dynamic characteristics of cytoophidia, we performed FRAP on four groups of hCTPS1 cytoophidia (Figure 2A and B). The intensity of FRAP ROI was normalized as $Normalized\ Intensity = \frac{I(non-bleach\ ROI)_{Pre-bleach,\ 0} - I(background)_0}{I(non-bleach\ ROI)_n - I(background)_n} \times [I(bleach\ ROI)_n - I(background)_n]$ (Warrington et al., 2022). The bleached ROI on cytoophidia induced by 20 μg/mL for 8 hours (low concentration and short time) before imaging recovered very quickly (Figure 2C). However, ROI in cells with hCTPS1 overexpression treated with DON in 100 μg/mL (higher concentration) recovered fluorescence slowly and ended at a lower intensity (Figure 2D; Supplemental Figure S1A).

By extending the DON treatment time to 25 hours, ROI can recover as soon as possible in a relatively short time (Figure 2E; Supplemental Figure S1B). The fluorescence intensity restored by bleaching ROI of cytoophidium-like condensates of hCTPS-EGFP cells is very small (Figure 2F; Supplemental Figure S1C)., There was a significant difference between hCTPS1-EGFP cytoophidium-like condensates and DON-induced hCTPS cytoophidia at low concentration and in a short time (Figure 2G).

This shows that DON-induced cytoophidia have very different dynamic characteristics from hCTPS-EGFP cytoophidium-like structure. DON-induced cytoophidia seem not assembled by simple force like hCTPS- EGFP cytoophidium-like condensates.

The bleached ROI gradually recovered throughout the ROI, rather than from any side of the ROI. Neither of the two ROIs moved to either side, nor were they far away or close to each other (Figure 2C). We observed that bleached hCTPS1 molecules in cytoophidia could exchange with free hCTPS1 molecules in the cytosol (Figure 2H).

The skeletal structure of hCTPS1 cytoophidium and its localization with hIMPDH2

In order to build a model to fit the dynamic equilibrium characteristics of cytoophidia, we obtained the super-resolution structures of hCTPS cytoophidia using stimulated emission depletion microscopy (STED). The images under conventional confocal microscopy could not show the structure inside cytoophidia, while the STED images revealed the super-resolution structure with a resolution of 50 to 70 nm (Figure 3A).

The super-resolution structure inside hCTPS cytoophidia was not homogeneous. Some parts of it were more condensed, while other parts are looser. It seemed that there were many tiny filaments inside, and tiny filaments in different orientations were constructed into a skeletal structure (Figure 3A; Supplemental Figure S2A). However, the super-resolution results were homogeneous inside hCTPS1-EGFP cytoophidium-like structure (Figure 3A). It is totally different between the structure of hCTPS cytoophidia and that of hCTPS1-EGFP.

These tiny filaments appear as the skeleton of hCTPS cytoophidia (Figure 3A and B). In vitro experiments show that CTPS can be assembled into filaments (Lynch et al., 2017; Zhou et al., 2019). Based on the in vitro and in vivo results, we envisioned a model to illustrate the skeletal structure of hCTPS cytoophidia (Figure 3B). The model can make FRAP results clearer. The dynamic equilibrium of assembly and disassembly occurs in the tiny filaments of hCTPS,

rather than the assembly and disassembly of the whole cytoophidia. FRAP on untreated and dispersive hCTPS1 signal resulted in fast recovery, which made us unable to capture the image after bleaching, which was similar to the image before bleaching (Supplemental Figure S2B).

After obtaining the super-resolution skeleton structures, we wanted to know the reason and function of this skeletal structure. There might be some unknown molecules in the space between hCTPS skeletons (Figure 3B). It was reported that IMPDH2 interacted with CTPS1 cytoophidia under DON treatment (Chang et al., 2018). Cytoophidia of hCTPS1 and hCTPS2 located together in 293T cells (Supplemental Figure S2C). IMPDH and CTPS are both part of the glutamine and NH_3 metabolic pathways (Supplemental Figure S2D). We overexpressed hCTPS1-EGFP^{A206K}, a monomer version of EGFP, and labeled IMPDH2 with Cy5 by immunofluorescence staining. Under DON treatment, IMPDH2 and hCTPS1 were colocalized spatially (Figure 3C). IMPDH2 and hCTPS1 were not exclusive, but were positioned mutually in each Z stack (Figure 3D). Therefore, IMPDH2 could be one of the molecules located between hCTPS1 skeletons.

When doing super-resolution imaging, there might be some influencing factors, such as the efficiency of antibodies, optical properties of fluorescent labeling, the steric hindrance of fluorescence proteins, and the influence of sample

preparation. To eliminate the effects of antibodies and Cy5, we used 293T cells with hCTPS1-miRFP670nano for live cell imaging. We performed immunofluorescence staining on DON-treated 293T cells to eliminate the effects of steric hindrance and overexpression. Both results showed skeletal structures (Figure 3A). To avoid the difference of optical properties between Cy5 and EGFP, we also performed immunofluorescence staining with Cy5 on hCTPS1-EGFP overexpressed 293T cells and signal obtained was from Cy5 (Figure 3A).

In addition, we performed immunofluorescence staining on SW480 cells cultured in glutamine free medium, which showed a skeletal structure (Figure 3A). Glutamine is the NH_3 donor in metabolic reaction. This means that the skeletal structure of hCTPS is not only a phenomenon induced by DON, but also a common structure of metabolic enzymes when cells are under metabolic stress. Without changing the super-resolution structure results, deconvolution of the STED images could improve their resolution and signal-to-noise ratio (Figure 3A; Supplemental Figure S2A).

CTPS granules with tentacles

We found that hCTPS1 could not only form cytoophidia, but also formed DON induced granules (Figure 1A). The movement of most granules was random walk like that of ordinary granules in cells (Figure 1B). Fortunately, when we observed live cells treated with DON, we found a filiform structure connected

between hCTPS1 granules (Figure 4A). We name these filiform structures connecting granules “tentacles”, and the main part of the granules is called the “granule body”. The tentacle slowly extended out of the granules body and retracted as quickly as a rubber band after reaching its longest length (Figure 4B).

We wanted to know the function of the granule tentacles. We found that tentacles were different from small granule bodies. When the tentacle stretched out, the granule body moved from one side of tentacle to the other side along the tentacle, and then tentacle retracted the granule body in the new location (Figure 4C). The movement of tentacle granules was different from that of non-tentacle granules. Granular tentacles are tiny structures that move granules (Figure 4D).

DISCUSSION

In this study, we use EGFP dimer tag to change the physical characteristics of hCTPS1 as the control group, and perform FRAP and STED to reveal the structure of cytoophidia. In addition, we observed hCTPS1 forms granules with tentacles.

CTPS 355H, which lies at the tetramer-tetramer interface, plays a critical role for CTPS polymerization. This mechanism for CTPS tetramer assembly of cytoophidia is more like actin filament than liquid droplets in cells assembled by physical forces (Banani et al., 2017; Zhang, 2020). However, when bleached ROI gradually restored its intensity, no treadmill phenomenon was observed, which means that the assembly mechanism of cytoophidia is different from that of actin filaments. Super-resolution STED imaging reveals the skeletal structure of cytoophidia.

The skeletal structure of cytoophidia provides a structural basis for the localization of other enzymes such as IMPDH. Both CTPS and IMPDH are related to glutamine and NH_3 metabolism. There may be dynamic interaction between CTPS, IMPDH and their substrates with microenvironment in skeletal cytoophidia. The skeletal structure may also provide elasticity for the bending or twisting of cytoophidia (Figure S1B). It was reported that cytoophidia are

related to regulation of IMPDH activity (Chang et al., 2015). Dynamic equilibrium of assembly and disassembly in subunit filaments may contribute to the reaction in the metabolic regulated microenvironment. CTPS moves between filament composition and free state.

In *C. crescentus,* a small amount of CTPS forms a bundle, while a large amount CTPS forms a splayed structure (Ingerson-Mahar et al., 2010). A large number of hCTPS transforms the morphology of CTPS bundles into complex structures. Cytoophidia are regulated by the level of cell crowding (Chang et al., 2022). The formation and maintenance of the skeletal cytoophidia may be related to cell crowding. Compartmentalization of enzymes takes many forms. Cytoophidia and hCTPS1 granules can exist in the same cells, with potential interaction and transformation. Tentacles also have orientation, just like cytoophidia.

MATERIALS AND METHODS

Cell culture

293T and SW480 were cultured in DMEM (SH30022.01, Hyclone) supplemented with 10% FBS (04–001; Biological Industries) in a humidified atmosphere containing 5% CO2 at 37°C. DON was dissolved in PBS. DON were added to cultured medium as described in individual experiments. DMEM without glutamine (C11960500BT, Gibco) replaced DMEM 8 hours before imaging.

Constructs and transfection

The pLV-hCTPS1-EGFP over-expression vector was kindly provided by Dr. Zhe Sun from ShanghaiTech University. mCherry, miRFP670nano replaced EGFP and $EGFP^{A206K}$ mutated back into EGFP using PCR and Gibson Assembly System (NEB). Cell transfection was done with PEI reagent (24765-1, Polysciences) according to instructions provided by the manufacturers. The sequences of oligonucleotides used in this study are listed in Supplemental Table S2.

Immunoblotting

Cells were harvested in lysis buffer (Containing 20mM Tris, 150mM NaCl and 1% Triton X-100; P0013J, Beyotime). Undissolved cell fraction was separated

by centrifugation at 12000 rpm for 10 min at 4°C and the supernatant were boiled in SDS-PAGE loading buffer for 10 min. Proteins in total cell lysates were separated by SDS-PAGE and transferred to PVDF membranes. Membranes were blocked in 5% nonfat milk and incubated with the appropriate primary antibodies. Protein bands were visualized through horseradish peroxidase (HRP) conjugated secondary antibody by ECL reagent (34577, ThermoFisher Scientific).

Immunofluorescence

Cells were fixed with 4% paraformaldehyde added into media for 25 min. Then the fixed cells were washed in 1xPBS for 3 times. Samples were incubated with appropriate primary antibodies (rabbit anti IMPDH2, Proteintech 12948-1-AP; rabbit anti CTPS, Proteintech 15914-1-AP) overnight at 4 °C, washed in PBS for 3 times. Samples were incubated with Cy5 conjugated secondary antibodies (donkey anti rabbit Cy5 conjugated antibody, Jackson 711-175-152) at room temperature for 1 hour (in dark), and washed with PBS for 3 times after incubation. Mountant for STED imaging (Figure 3A, C, D; Figure S2A) was Prolong™ Diamond Antifade (Invitrogen. P36965). Mountant for confocal imaging (Figure 1H) was HardSet Mounting Medium with DAPI (VECTASHIELD, H-1500)

Microscopy

Images (Figure 1A, B; Figure 2C; Figure 4A, C; Figure S1A, B, C; Figure S2B) were acquired under 100× objectives on a confocal microscope (Nikon CSU-W1 SoRa). Confocal images and super-resolution images (Figure 3A, C, D; Figure S2A) were acquired under 100× objectives on a STED confocal microscope (Leica TCS SP8 STED 3X). Images (Figure S2C) were acquired under 63× objective on Lattice SIM microscope (Zeiss Elyra 7) with wide-field mode. Confocal images (Figure 1H) were acquired under 63× objective on confocal microscope (Zeiss LSM 980 Airyscan2).

Live imaging

293T cells transfected with hCTPS1-mCherry and hCTPS1-miRFP670nano constructs were cultured on glass bottom culture dishes (C8-1.5H-N, Cellvis) with medium and maintained at 37 °C when live imaging was performed.

Image analysis

Fluorescence images was analyzed with the software IMAGEJ (NIH, Bethesda, MD, USA). The ROIs of bleached region for intensity measurement in Figure 2 were selected and measured manually with IMAGEJ. The FRAP curve unpaired t test was analyzed with Graph Prism 8. The deconvolution of STED images shown in Figure 3 was analyzed by lighting algorithm of Leica LAS X. The 3D model in Figure 3 was analyzed by Leica LAS X. The length of tentacles in figure 4 was measured manually with IMAGEJ. Quantity data was collected with

Microsoft Excel.

Flow cell analysis

The flow cell analyzer used was LSRFortessa X20 (BD). Flow cell data was analyzed with FlowJo 10.4 software. Data was collected with Microsoft Excel.

ACKNOWLEDGEMENTS

We thank the he Molecular Imaging Core Facility (MICF) at the School of Life Science and Technology, ShanghaiTech University for providing technical support. This work was supported by grants from Ministry of Science and Technology of China (No. 2021YFA0804700), National Natural Science Foundation of China (No. 31771490), Shanghai Science and Technology Commission (No. 20JC1410500) and the UK Medical Research Council (grant nos. MC_UU_12021/3 and MC_U137788471) for grants to J.L.L.

AUTHOR CONTRIBUTIONS

Y. Fang and J-L. Liu conceived the project. Y. Fang designed experiments. Y. Fang, Y-L. Li and X. Li performed experiments. Y. Fang analyzed the data. Y. Fang wrote the original manuscript. Y. Fang, Y-L. Li, X. Li and J-L. Liu revised the manuscript.

REFERENCES

Banani, S.F., Lee, H.O., Hyman, A.A., and Rosen, M.K. (2017). Biomolecular condensates: organizers of cellular biochemistry. Nat Rev Mol Cell Biol *18*, 285-298.

Brangwynne, C.P., Eckmann, C.R., Courson, D.S., Rybarska, A., Hoege, C., Gharakhani, J., Julicher, F., and Hyman, A.A. (2009). Germline P granules are liquid droplets that localize by controlled dissolution/condensation. Science *324*, 1729-1732.

Chang, C.C., Keppeke, G.D., Sung, L.Y., and Liu, J.L. (2018). Interfilament interaction between IMPDH and CTPS cytoophidia. FEBS J *285*, 3753-3768.

Chang, C.C., Lin, W.C., Pai, L.M., Lee, H.S., Wu, S.C., Ding, S.T., Liu, J.L., and Sung, L.Y. (2015). Cytoophidium assembly reflects upregulation of IMPDH activity. J Cell Sci *128*, 3550-3555.

Chang, C.C., Peng, M., Zhong, J., Zhang, Z., Keppeke, G.D., Sung, L.Y., and Liu, J.L. (2022). Molecular crowding facilitates bundling of IMPDH polymers and cytoophidium formation. Cell Mol Life Sci *79*, 420.

Chen, K., Zhang, J., Tastan, O.Y., Deussen, Z.A., Siswick, M.Y., and Liu, J.L. (2011). Glutamine analogs promote cytoophidium assembly in human and Drosophila cells. J Genet Genomics *38*, 391-402.

Ingerson-Mahar, M., Briegel, A., Werner, J.N., Jensen, G.J., and Gitai, Z. (2010). The metabolic enzyme CTP synthase forms cytoskeletal filaments. Nat Cell Biol

12, 739-746.

Ji, Y., Gu, J., Makhov, A.M., Griffith, J.D., and Mitchell, B.S. (2006). Regulation of the interaction of inosine monophosphate dehydrogenase with mycophenolic Acid by GTP. J Biol Chem *281*, 206-212.

Liu, J.-L. (2010). Intracellular compartmentation of CTP synthase in Drosophila. Journal of Genetics and Genomics *37*, 281-296.

Liu, J.L. (2016). The Cytoophidium and Its Kind: Filamentation and Compartmentation of Metabolic Enzymes. Annu Rev Cell Dev Biol *32*, 349-372.

Lynch, E.M., Hicks, D.R., Shepherd, M., Endrizzi, J.A., Maker, A., Hansen, J.M., Barry, R.M., Gitai, Z., Baldwin, E.P., and Kollman, J.M. (2017). Human CTP synthase filament structure reveals the active enzyme conformation. Nat Struct Mol Biol *24*, 507-514.

Noree, C., Sato, B.K., Broyer, R.M., and Wilhelm, J.E. (2010). Identification of novel filament-forming proteins in Saccharomyces cerevisiae and Drosophila melanogaster. J Cell Biol *190*, 541-551.

Shaner, N.C., Steinbach, P.A., and Tsien, R.Y. (2005). A guide to choosing fluorescent proteins. Nat Methods *2*, 905-909.

Warrington, S.J., Strutt, H., and Strutt, D. (2022). Use of Fluorescence Recovery After Photobleaching (FRAP)Fluorescence Recovery after Photobleaching (FRAP) to Measure In Vivo DynamicsDynamics of Cell Junction–Associated Polarity Proteins. In Cell Polarity Signaling: Methods and Protocols, C. Chang, and J. Wang, eds. (New York, NY: Springer US), pp. 1-30.

Zhang, H. (2020). The glassiness of hardening protein droplets. Science *370*, 1271-1272.

Zhou, X., Guo, C.J., Chang, C.C., Zhong, J., Hu, H.H., Lu, G.M., and Liu, J.L. (2021). Structural basis for ligand binding modes of CTP synthase. Proc Natl Acad Sci U S A *118*.

Zhou, X., Guo, C.J., Hu, H.H., Zhong, J., Sun, Q., Liu, D., Zhou, S., Chang, C.C., and Liu, J.L. (2019). Drosophila CTP synthase can form distinct substrate- and product-bound filaments. J Genet Genomics *46*, 537-545.

FIGURES 1-4

Figure 1. Assembly of CTPS filaments into cytoophidia.

(A) hCTPS1 forms granules in the same cell that coexist with hCTPS1 cytoophidia. The arrow head points out the granule (B) The trajectory of hCTPS1 granules is a random walk. For DON treatment, 20 μg/mL DON in PBS solution was added into fresh DMEM media 8 to 25 hours before living cell imaging. (C) hCTPS1-EGFP forms cytoophidium-like structures by simple force between EGFP. The arrangement from hCTPS1 filament to hCTPS cytoophidia is the problem that need to be solved. (D) The quantities of transfected over-expression hCTPS in 293T cells were measured respectively. (E and F) The transfection efficiencies were quantified respectively. (G) Estimated ratio of exogenous hCTPS1 to endogenous hCTPS. (H) hCTPS cytoophidia can be induced by DON treatment. hCTPS1-EGFP can form cytoophidium-like structure, which is wider and larger than hCTPS cytoophidium. hCTPS1^{H355A}-EGFP cannot form cytoophidia-like structure. For DON treatment, 20 μg/mL DON (PBS solution) was added into fresh DMEM media 8 hours before fixation. Scale bars, 10 μm (A, B) and 20 μm (H).

424

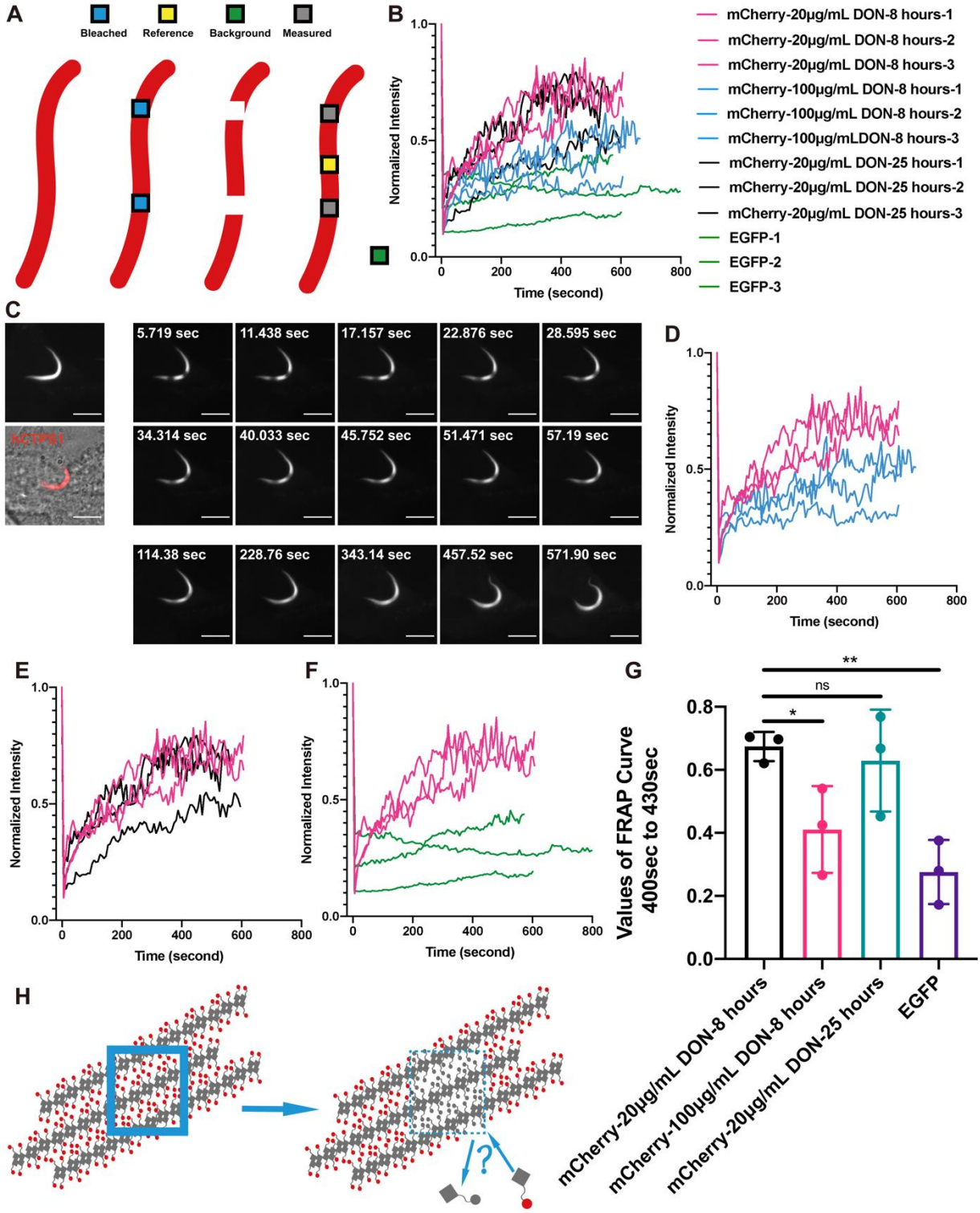
A
Bleached
Reference
Background
Measured
B
Normalized Intensity
Time (second)
mCherry-20μg/mL DON-8 hours-1
mCherry-20μg/mL DON-8 hours-2
mCherry-20μg/mL DON-8 hours-3
mCherry-100μg/mL DON-8 hours-1
mCherry-100μg/mL DON-8 hours-2
mCherry-100μg/mLDON-8 hours-3
mCherry-20μg/mL DON-25 hours-1
mCherry-20μg/mL DON-25 hours-2
mCherry-20μg/mL DON-25 hours-3
EGFP-1
EGFP-2
EGFP-3
C
5.719 sec
11.438 sec
17.157 sec
22.876 sec
28.595 sec
34.314 sec
40.033 sec
45.752 sec
51.471 sec
57.19 sec
114.38 sec
228.76 sec
343.14 sec
457.52 sec
571.90 sec
D
E
F
G
Values of FRAP Curve 400sec to 430sec
ns
mCherry-20μg/mL DON-8 hours
mCherry-100μg/mL DON-8 hours
mCherry-20μg/mL DON-25 hours
EGFP
H

425

426

Figure 2. Dynamic equilibrium of cytoophidia.

(A) ROIs were used for bleaching, measurement and standardization data. (B) Normalized intensity curves of FRAP results in different groups were merged. (C) Living cell images of FRAP on hCTPS1-mCherry cytoophidia induced by 20 μg/mL DON for 8 hours. (D) Comparison of FRAP curve on hCTPS1-mCherry between 20 μg/mL DON for 8 hours and 100 μg/mL DON for 8 hours. (E) Comparison of FRAP curve on hCTPS1-mCherry between 20 μg/mL DON for 8 hours (pink curve) and 20 μg/mL DON for 25 hours (black curve). (F) Comparison of FRAP curve between hCTPS1-mCherry cytoophidia (pink curve) induced by DON and hCTPS1-EGFP cytoophidium-like structures (green curve). (G) Analysis of the level and speed of fluorescence recovery *, p-value<0.05; **, p-value<0.01; ns, no significant difference. (H) It does not fit the results of FRAP images if hCTPS cytoophidia are compact or condensed. A new model is needed to illustrate the recovery of bleached fluorescence of cytoophidia. The intensity of FRAP ROI was normalized as $Normalized\ Intensity = \frac{I(non-bleach\ ROI)_{Pre-bleach,\ 0} - I(background)_0}{I(non-bleach\ ROI)_n - I(background)_n} \times [I(bleach\ ROI)_n - I(background)_n]$. Scale bars, 10 μm (C).

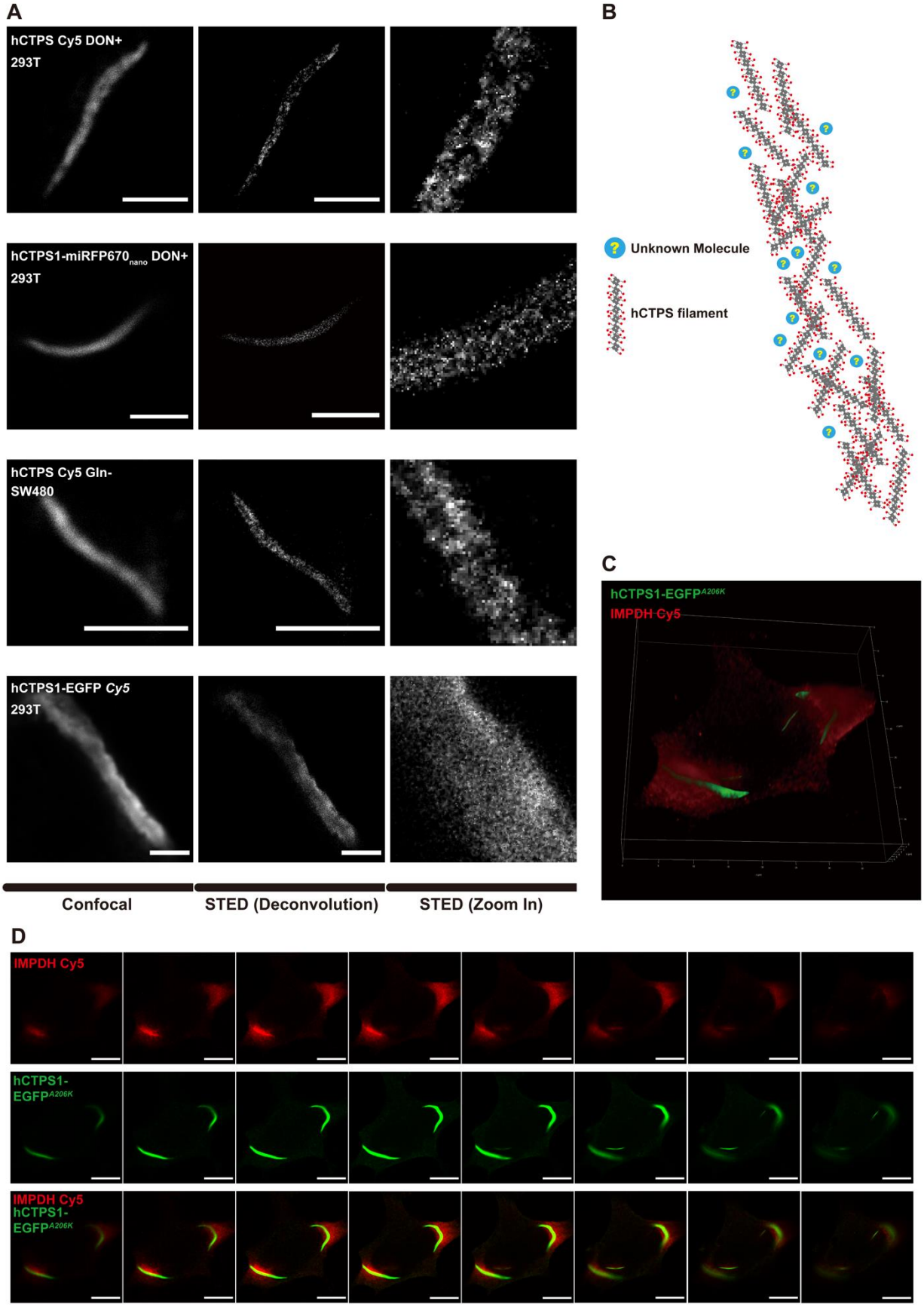
A
hCTPS Cy5 DON+
293T
hCTPS1-miRFP670nano DON+
293T
hCTPS Cy5 Gln-
SW480
hCTPS1-EGFP Cy5
293T
Confocal
STED (Deconvolution)
STED (Zoom In)
B
Unknown Molecule
hCTPS filament
C
hCTPS1-EGFPA206K
IMPDH Cy5
D
IMPDH Cy5
hCTPS1-
EGFPA206K
IMPDH Cy5
hCTPS1-
EGFPA206K

445

Figure 3. The skeletal structure of hCTPS1 cytoophidium and its localization with hIMPDH2

(A) Confocal,STED with deconvolution and zoom-in images of cytoophidia from the following groups: 1) hCTPS1/2 cytoophidia (Cy5 antibody stained) induced by DON in fixed 293T cells, 2) hCTPS1-miRFP670nano cytoophidia induced by DON in live 293T cells, 3) hCTPS1/2 (Cy5 stained) cytoophidiainduced by glutamine deprivation in fixed SW480 cell and 4) hCTPS1/2 (Cy5 stained)-cytoophidium-like structure in live 293T (hCTPS1-EGFP overexpression) cell. For SW480 culture, DMEM without glutamine replaced DMEM 8 hours before fixed. For DON treatment, DON (PBS solution) was added into fresh DMEM media 8 to 25 hours before living cell imaging or 8 hours before being fixed. Scale bars, 3 μm. (B) The arrangement model of hCTPS filaments into cytoophidia. (C) In 293T cells, hCTPS1-EGFP^{A206K} was colocalized with DON induced IMPDH2(Cy5 stained). (D) In each slice along Z stacks, hCTPS1-EGFP^{A206K} and IMPDH2 (Cy5 stained) are localized to each other. Scale bars, 3 μm 10 μm.

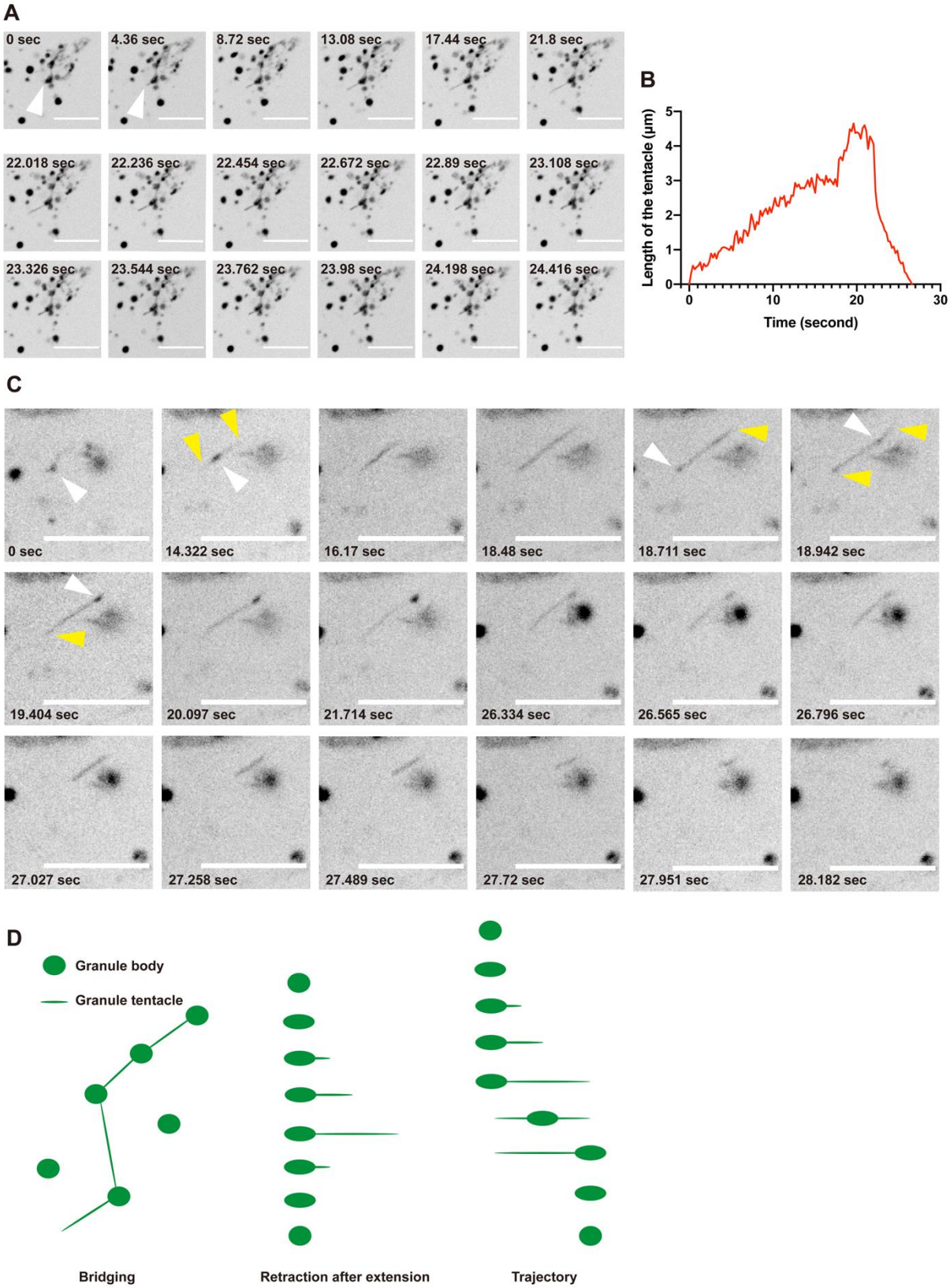
A
0 sec
4.36 sec
8.72 sec
13.08 sec
17.44 sec
21.8 sec
22.018 sec
22.236 sec
22.454 sec
22.672 sec
22.89 sec
23.108 sec
23.326 sec
23.544 sec
23.762 sec
23.98 sec
24.198 sec
24.416 sec
B
Length of the tentacle (μm)
Time (second)
C
0 sec
14.322 sec
16.17 sec
18.48 sec
18.711 sec
18.942 sec
19.404 sec
20.097 sec
21.714 sec
26.334 sec
26.565 sec
26.796 sec
27.027 sec
27.258 sec
27.489 sec
27.72 sec
27.951 sec
28.182 sec
D
Granule body
Granule tentacle
Bridging
Retraction after extension
Trajectory

463

Figure 4. CTPS granules with tentacles.

(A) Tentacles connect hCTPS1 granules. Tentacles extend and retract.Arrow head indicates the tentacle. (B) Tentacles extend slowly and retract rapidly after reaching the maximum length. (C) hCTPS1 granules move from one side to the other along the tentacles. Yellow arrow heads indicate the tentacles. White arrow heads indicate the granules. (D) hCTPS1 granule tentacles have three different behaviors and characteristics, bridging, retraction after extension, and the trajectory of hCTPS1 granule movement. For DON treatment, DON (PBS solution) was added to fresh DMEM media 8 to 25 hours before living cell imaging. Scale bars, 10 μm (A, C).